

We are IntechOpen, the world's leading publisher of Open Access books Built by scientists, for scientists

6,900

Open access books available

185,000

International authors and editors

200M

Downloads

Our authors are among the

154

Countries delivered to

TOP 1%

most cited scientists

12.2%

Contributors from top 500 universities



WEB OF SCIENCE™

Selection of our books indexed in the Book Citation Index
in Web of Science™ Core Collection (BKCI)

Interested in publishing with us?
Contact book.department@intechopen.com

Numbers displayed above are based on latest data collected.
For more information visit www.intechopen.com



On the Friction of Oil-Impregnated Sintered Bearings

Naofumi Hiraoka

Abstract

Oil-impregnated sintered bearings are widely used in various products. Friction reduction in them is still a large target for the related industries. In those bearings, lubricating oil exudes from the porous bearing body and lubricates the shaft and bearing surfaces. However, the amount of oil in those sliding areas is often insufficient leading to an unsatisfactory friction. Oil wettability of the shaft surfaces was found to have a large effect on the friction of those bearings. Low oil-wettable shaft could retain a larger amount of oil in the bearing clearances and indicated lower friction than highly wettable shaft. This is because a large contact-angle hysteresis between the oil and the low-wettable shaft surface allows the retention of large oil droplets in the bearing clearances. The control of oil-wettability of the shaft surface could be an effective means of reducing friction for oil-impregnated sintered bearings.

Keywords: friction, lubrication, wettability, surface tension, contact angle, surface treatment

1. Introduction

Oil-impregnated sintered bearings are widely used in various products, especially in motor vehicles and office automation (OA) equipment [1, 2]. For example, they are used in more than 30 parts of automobiles [3]. In these bearings, lubricating oil exuding from the porous bearing body to the sliding surface lubricates the shaft and the bearing. The exudation occurs due to thermal expansion of the oil volume by frictional heat, the “pumping effect” caused by negative pressure in the lubricating oil film [2, 4], and capillary force. Due to such mechanisms, these bearings are expected to have a long service life and relatively low friction without an external oil supply.

Generally, friction of oil-impregnated sintered bearings is larger than fully lubricated bearings, because they are often under boundary lubrication condition. These bearings are often used in relatively small parts, and their friction loss is a serious issue because of small power consumptions allowed for such parts. Frictional noise is also a problem, especially for OA equipment, which is related to lubrication conditions. To improve the lubrication conditions and reduce the friction of these bearings has been the challenge for many researchers and is still a major problem today.

In this chapter, lubrication conditions of oil-impregnated sintered bearings are roughly explained, and the effects of oil wettability of the shaft surface on improving the lubrication conditions are discussed [5].

2. Lubrication conditions

Figure 1 shows the optical microscopic image of the oil-impregnated sintered bearing surface. Many pores and gaps among the grains could be found in sintered metal body. Lubricating oil is impregnated in these pores and gaps usually using vacuum condition. As described above, lubricating oil exudes from the porous body to the sliding surface in some ways during sliding and lubricates the shaft and bearing surface. The schematic view of the shaft and bearing is shown in **Figure 2**. As can be considered from these oil supply mechanisms, oil amount in the bearing gap is usually smaller than fully lubricated bearings and sometimes insufficient for good lubrication.

In addition to oil supply problem, there are some features that make low friction difficult to realize. Some exuded oil returns into the pores of the bearing body by capillary force and also leading to insufficient oil on the sliding surface [4, 6]. The porous surface of the bearing means a reduction in the load area, which lowers the loading capacity of the bearing. Although fluid lubrication was reported to be possible for oil-impregnated sintered bearings especially under large sliding speed conditions [7], the sliding area of the bearing is often under a boundary or mixed

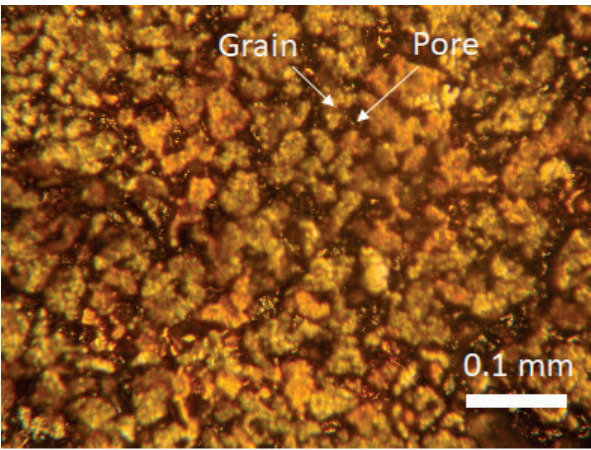


Figure 1.
Optical microscopic image of oil-impregnated sintered bearing surface. Arrows indicate the example of a grain and a pore.

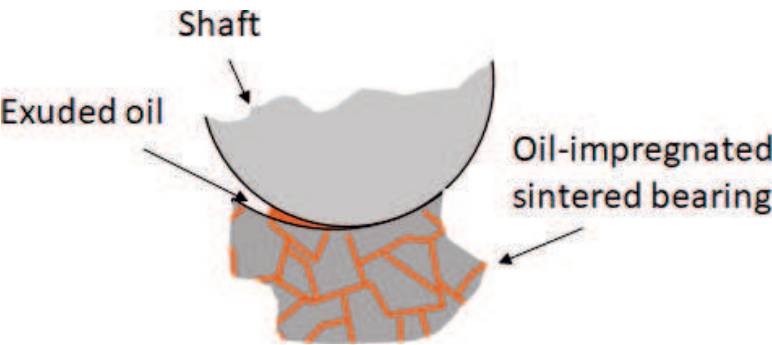


Figure 2.
Schematic view of shaft and bearing.

lubrication condition [6] due to the reasons mentioned above, resulting in large bearing friction.

To improve the bearing friction under such lubrication conditions, solid lubricants are sometimes added to the bearing materials, or an oiliness agent (e.g., stearic acid) is added to the impregnated oil [2, 4, 8]. However, the friction of oil-impregnated sintered bearings is generally higher than that of fully lubricated bearings [6].

3. Oil wettability of shaft surfaces

Metal surfaces generally show good wettability with oils. Lubricating oil could spread easily into sliding area and stay there stably due to this property. This realizes good lubrication condition for machines.

There is a report that a low oil-wettable surface showed low friction due to the slip between the oil and the surface especially under fluid lubrication condition [9]. Some processing, coating, doping, etc., on the surface is usually necessary to provide low oil wettability to metal surfaces and needs additional cost. Recently, a novel grinding method was reported to give processed surface hydrophilicity [10], which probably could give low oil wettability to the surface at low cost. Though such techniques will possibly generalize low oil-wettable shafts, it seems that providing low oil wettability to the metal surfaces is not widely practiced so far to reduce the friction considering the benefits of good wettability to the lubricity described above and cost-effectiveness.

However, as will be shown below, imparting the low oil wettability to the shaft can be a relatively simple way to basically improve the lubrication condition for oil-impregnated sintered bearings.

4. Friction of oil-impregnated sintered bearings

4.1 Friction measurement for shafts with different wettability

Friction coefficients of oil-impregnated sintered bearings with stainless steel shafts were measured. Specimens used are described in **Table 1**. The oil-impregnated sintered bearing used is commercially available mainly for OA equipment, and the size was relatively small.

Bearing	Fe-Cu-based commercial oil-impregnated sintered bearing Oil content: 20.4~20.8% Bore: 4.009 mm. Width: 3 mm
Impregnated oil	Synthetic oil Kinematic viscosity: 42.9 mm ² /s@40°C Surface tension: 25 mN/m@20°C
Noncoated shaft	Material: JIS SUS420J2 hardened stainless steel Diameter: 3.996~3.997 mm Surface roughness: Ra 0.022~0.028 μm
PTFE-coated shaft	Material: JIS SUS420J2 hardened stainless steel + PTFE transfer coating Diameter: 3.996~3.997 mm Surface roughness: Ra 0.024~0.028 μm

Table 1.
Specimen descriptions.

A simple test rig shown in **Figure 3** was used to measure the frictional torque of the bearings. The bearing was inserted and fixed in a ring-shaped weight. The frictional torque T was measured and converted to the friction coefficient μ by

$$\mu = T/(RW) \quad (1)$$

where R is a radius of the bearing bore, and W is the weight load.

Tests were conducted under a weight load of 6.7 N and at a shaft rotation speed of 100–800 rpm. Average frictional torque values were measured every 10 s for each 100-rpm increase in speed. Note that bearing frictional torque is usually different from that of the shaft.

Two types of the shafts: noncoated and PTFE coated stainless steel shafts in **Table 1**, were evaluated. The noncoated stainless steel shafts were used for oil wettability shaft. For the low wettability shaft, PTFE (polytetrafluoroethylene) transfer film coated stainless steel shafts were used. The PTFE block was lightly pressed against the rotating shaft surface and then gently wiped with a nonwoven fabric to make a PTFE transfer coating. As PTFE is known for its low surface energy and ability to make a transfer film on the counter surface by sliding [11], the shaft surface made by this method was expected to have low oil wettability.

Surface roughness was not much different between the stainless steel shaft and the PTFE coated shaft surface as shown in **Table 1**. The shaft diameter measurement by a micrometer before and after application of the coating indicated the PTFE coating thickness was less than 1 μm , though exact thickness was unknown. The past literatures have showed the PTFE transfer film thickness was in the order of several nm [12–14].

Oil droplets on the shafts about 10 s after being deposited there were shown in **Figure 4**. Colors of the droplets appeared a little different between the shafts, but it was due to the oil droplet thickness. Contact angle for noncoated shaft was much lower than that of the PTFE-coated shaft. The oil droplet on the noncoated shaft subsequently spread to cover the wide range of the shaft surface, while that on the PTFE-coated shaft retained its original droplet shape. This clearly indicates the lower oil wettability of the PTFE-coated shaft surface, as compared to that of the noncoated shaft surface.

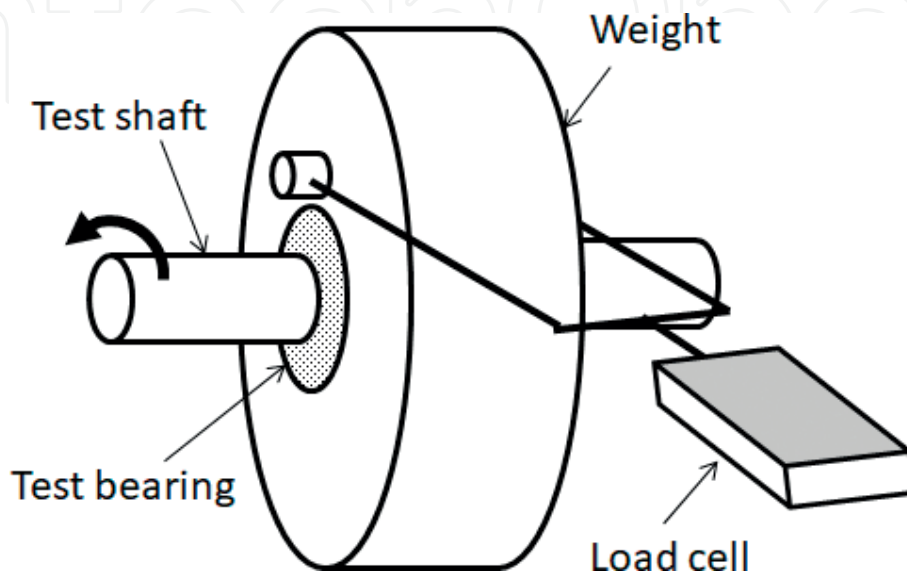


Figure 3.
Schematic view of bearing friction test rig.

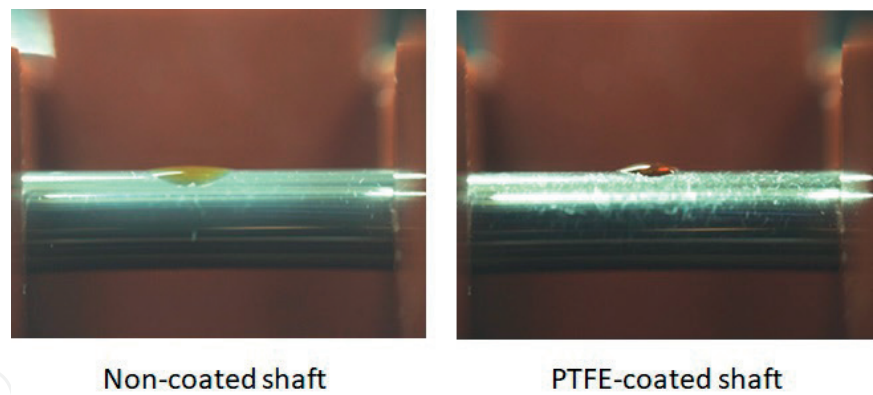


Figure 4.
Oil droplets on the shafts.

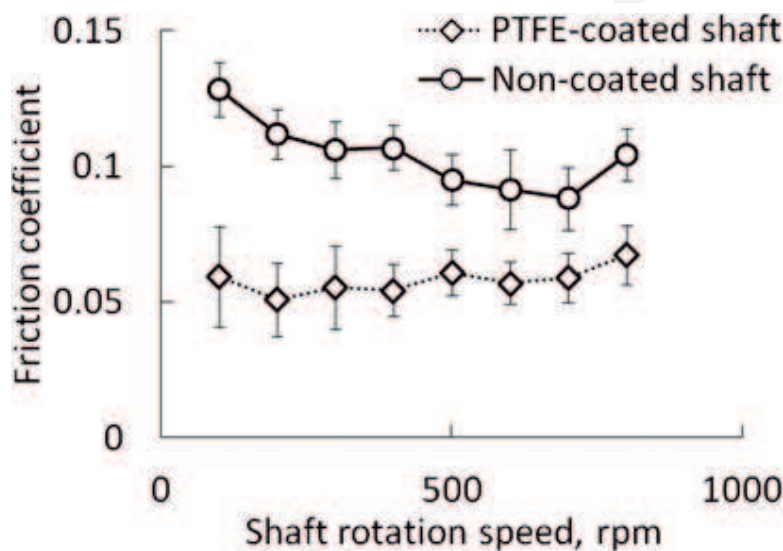


Figure 5.
Friction coefficients of the bearings. Error bars indicate the standard error of the mean.

Figure 5 shows the friction coefficients of the bearings calculated by Eq. (1) with PTFE-coated and noncoated shafts. Error bars indicate the standard error of the means of five time test data for each shaft. The PTFE-coated shaft indicated a friction coefficient 20–50% lower than that of the noncoated shaft on average. Lubrication condition was presumed to be boundary lubrication, because friction coefficients are not largely dependent on shaft rotation speed.

Figure 6 shows metallurgical microscopic (Olympus BHMJ, Japan) images of typical shaft and bearing surfaces before and after the tests. As compared to the intact shaft surface which could be estimated from the nonsliding area, wear marks were found on the sliding areas of shafts and bearings of both non- and PTFE-coated shaft tests. Comparing these surfaces, those for the PTFE-coated shaft test showed comparatively milder wear appearance.

4.2 Oil amount in the bearing clearance and the shaft wettability

As was described, one of the big problems for the lubricity of oil-impregnated sintered bearings is poor oil supply to the sliding surfaces. We focused on the oil amount on the shaft and in the bearing clearance first as a cause of the friction reduction of the PTFE-coated shaft.

Figure 7 shows oil deposition on the shafts pulled out from the bearings. Before the shafts were pulled out and the photos were taken, the shafts were rotated

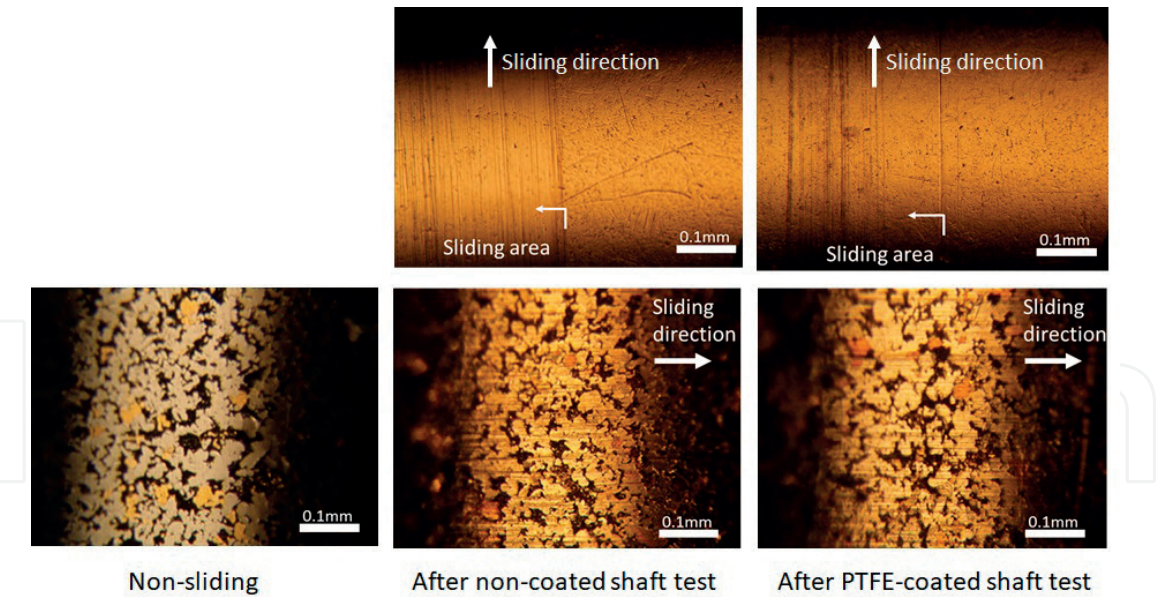


Figure 6.
Shaft and bearing surfaces before and after the tests. Upper: shaft surfaces. Lower: bearing surfaces.

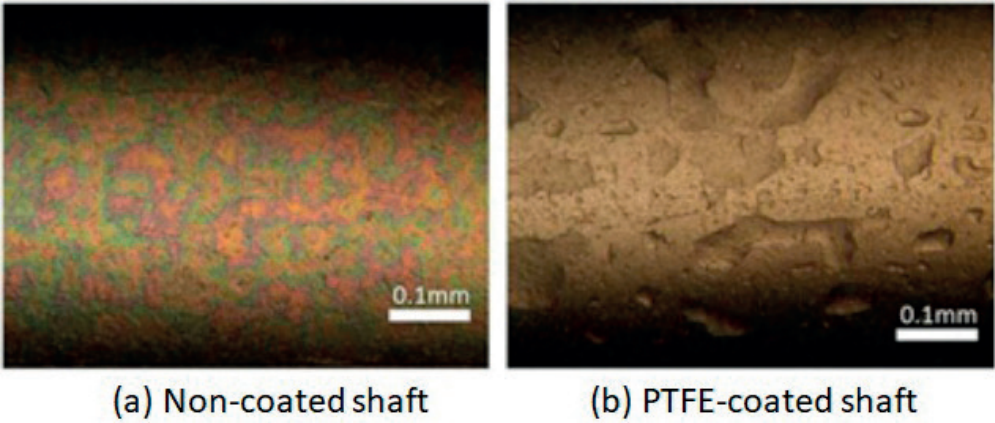


Figure 7.
Oil deposition on the shafts.

several times by hand in the bearings. There were many oil droplets on the PTFE-coated shaft surface, while only interference patterns of a thin film of oil were found on the noncoated shaft surface, which suggested the richer oil amount for the PTFE-coated shaft and bearing pair. However, very thin oil film on the non-coated shaft might not have suggested the less oil amount directly, because it could be due to rapid oil spreading on the shaft before the photos were taken. Next, the oil in the bearing clearances was observed directly to clarify.

The projections of the bearing clearances with fixed shafts were taken with a profile projector (Mitsutoyo PJ-3000F, Japan) and were shown in **Figure 8(a-1)** and **(b-1)**. The configuration of the projector and the tested bearing is shown in **Figure 9**.

The shafts were rotated by hand several times prior to the observation. Then the shafts were rotated about 45 degrees for several seconds from the initial positions. **Figure 8(a-2)** and **(b-2)** shows the photos at that time. Though clear individual figures of oil droplets were lacking, because they were deposited not only in the plane direction but also in the depth direction, there were many and large oil droplets indicated by arrows in the clearance between the PTFE-coated shaft and the bearing, while only a few and small droplets on the noncoated shaft. The difference between (a) and (b) in **Figure 7** must have been caused by this.

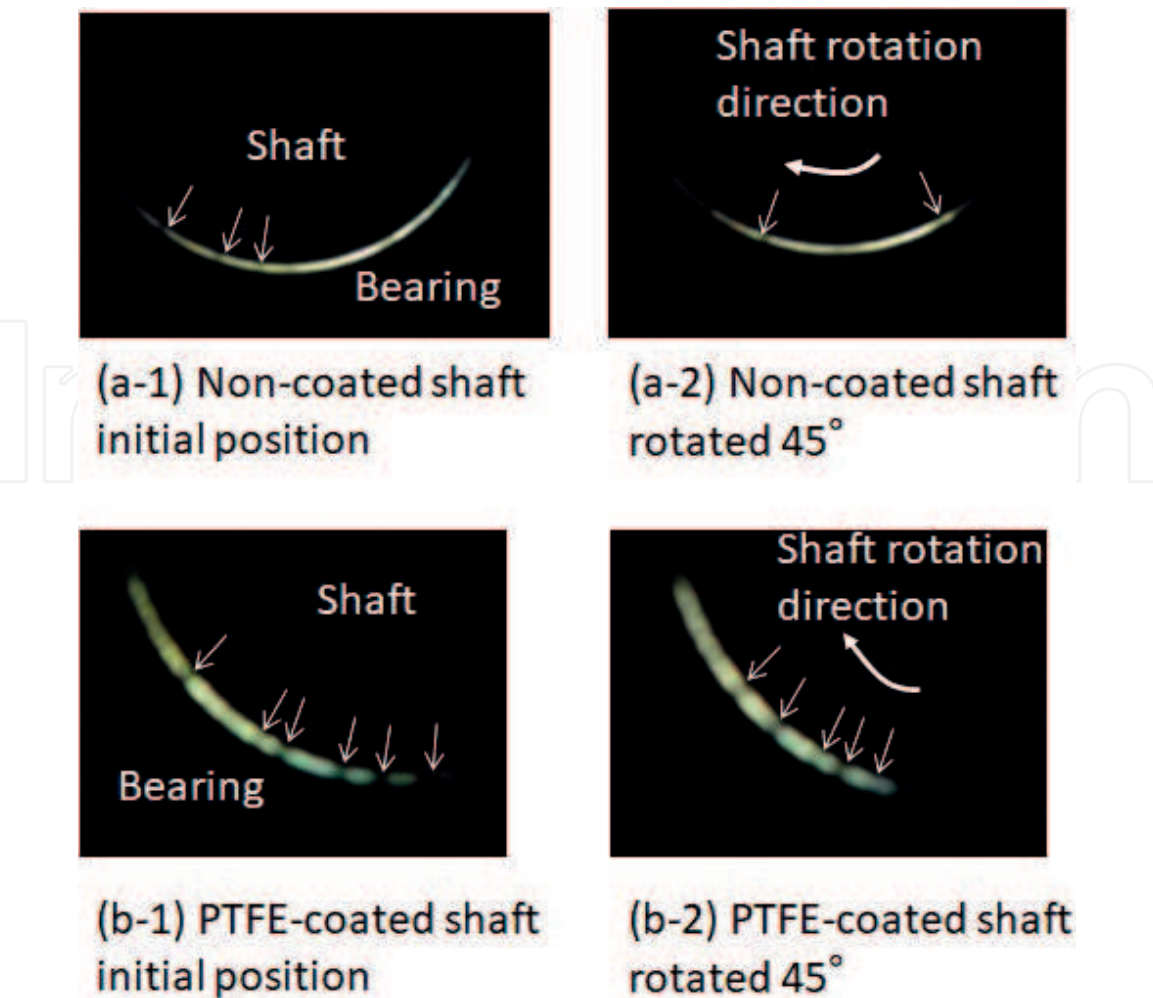


Figure 8.
Bearing clearance projections. Arrows indicate the position of the droplets.

In addition to the large amount of the oil droplets, droplets on the PTFE-coated shaft were observed to move together with shaft rotation, which leads to oil circulation in the clearance, from the moving images taken during the 45° shaft rotation.

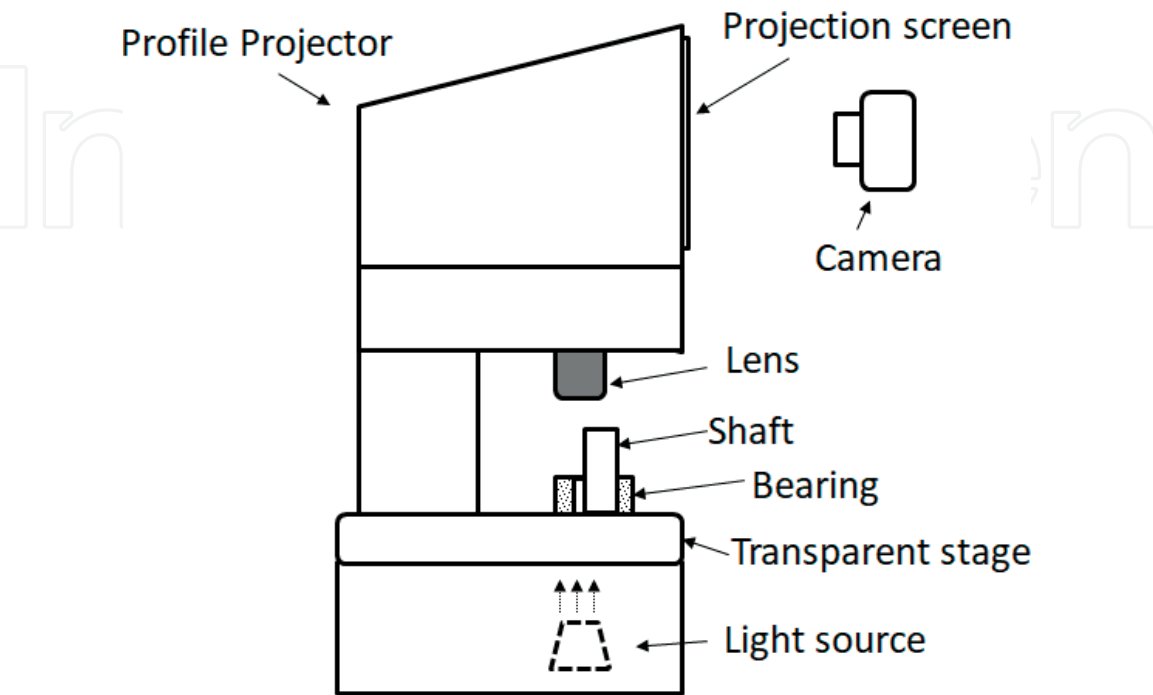


Figure 9.
Configuration of the projector and the tested bearing.

New droplets were observed to emerge from the edge of the clearance and move in the same manner, that is, oil exudation in the clearance for the PTFE-coated shaft was clearly observed. No conspicuous motion of the oil droplets was observed in the clearance for the noncoated shaft during shaft rotation.

To summarize, much larger amount of oil was retained in the bearing clearance for the PTFE-coated shaft (i.e., low wettable shaft) than that for the noncoated shaft (i.e., highly wettable shaft), and oil circulation in the bearing clearance (along with shaft rotation) was observed for the PTFE-coated shaft. This means the oil-rich and secure oil exuding condition for the sliding area of the PTFE-coated shaft and relatively oil-poor condition for the noncoated shaft. Smaller friction of the PTFE-coated shaft was probably attributable to this oil-rich condition.

The past literature has showed that the oil-poor condition increases the friction of sintered bearings [15]. More frequent solid–solid contact could occur for a less amount of oil condition in the sliding area, and thus was naturally one of the reasons for larger friction of the noncoated shaft. The oil-rich condition leads to the lower friction of the PTFE-coated shaft.

4.3 Other effects to cause the difference in friction

In this section, possible mechanisms other than those mentioned in the previous section that caused the difference in friction are discussed.

One of the effects to be noticed especially for poor oil condition is capillary force. Less amount of oil supply to the sliding area would pose synergistic effect of poor lubricity and capillary force on friction increase to the bearing.

Figure 10 shows the diagram of the oil meniscuses in the bearing clearance. Capillary force (F) is generated by negative Laplace pressure in the oil film. Assume that the oil filled the clearance plane symmetrically. Ignoring the effects of hydrodynamic force, the bearing end effect and oil droplets in the rest of the bearing clearance, and approximating zero contact angles between the oil and bearing/shaft

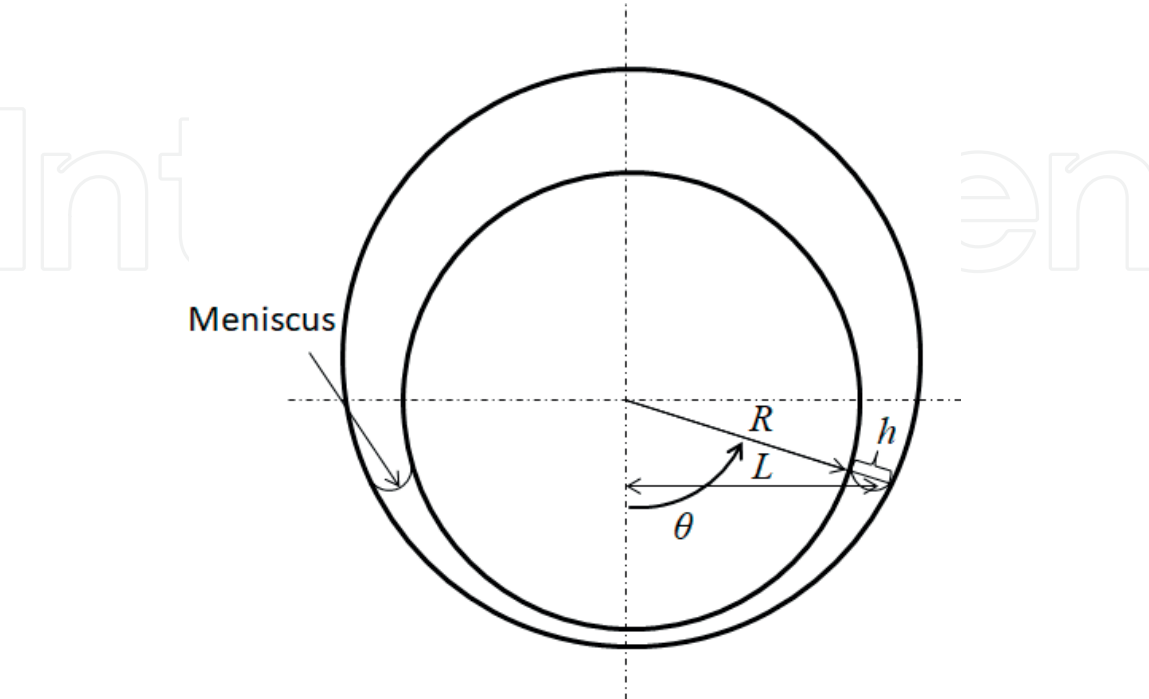


Figure 10.
Diagram of oil meniscuses in bearing clearance.

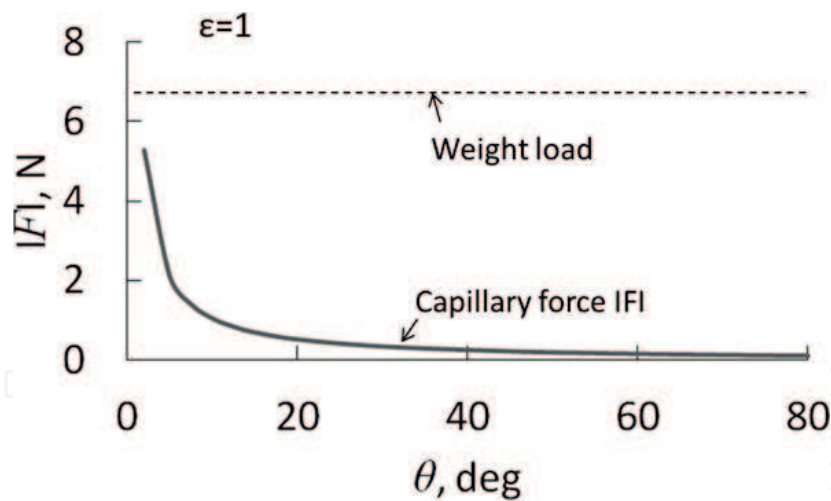


Figure 11.
Calculated capillary force.

surface (the curvature of the meniscus to be $-h/2$), the capillary force could be estimated as follows:

$$F = 2LB\Delta p = -2LB\gamma/(h/2) \tag{2}$$

$$h \approx c(1 - \epsilon\cos\theta) \tag{3}$$

$$L = R\sin\theta \tag{4}$$

where, B is the bearing width, Δp is the Laplace pressure, γ is the surface tension of the oil, c is the bearing radial clearance, ϵ is the eccentricity ratio, and R is the shaft radius.

Figure 11 shows the calculated capillary force along with $\epsilon = 1$ (which denotes the contact of the shaft and the bearing), $c = 6.5 \mu\text{m}$, and the tested bearing dimensions. $|F|$ increases with a decrease in θ continuously and increases rapidly at an angle of 10° or less. **Figure 11** indicates that smaller the oil amount is, larger the capillary force becomes and consequently friction becomes larger.

To estimate the effect of the capillary force on the bearing friction, assume the oil filled by $\theta = \pm 30^\circ$ for the noncoated shaft and $\theta = \pm 80^\circ$ for the PTFE-coated shaft in the bearing clearance, respectively. Using Eqs. (2)–(4), F is -0.34 N for $\theta = \pm 30^\circ$ and -0.11 N for $\theta = \pm 80^\circ$. Thus, the sum of the loads by weight (6.7 N) and capillary force, the actual load, for the PTFE-coated shaft, is 3% less than that of the noncoated shaft. Considering that friction reduction rate was 20–50%, this load difference would not be negligible. In considering a smaller θ , $|F|$ increases rapidly and the actual load for a noncoated bearing becomes large. Hence, the capillary force due to less oil could be the part of the larger friction.

Another possible mechanism of lower friction for the PTFE-coated shaft was slippage between the oil film and the shaft surface. A hydrophobic surface may cause boundary slip—a measure of relative fluid velocity at the solid-fluid interface [9, 16, 17] that leads to low friction under boundary lubrication. This effect was examined by the following friction tests.

The tests were conducted by using a ball-on-plate reciprocating friction tester for PTFE-coated and noncoated plates in the same oil as impregnated oil. **Table 2**

Ball	Material: JIS SUS304 stainless steel Diameter: 10 mm
Plate	Material: JIS SUS304 stainless steel Surface roughness: Ra 0.2 μm
Load	1.6 N
Stroke	30 mm
Sliding speed	30 mm/s

Table 2.
Test conditions and materials for ball-on-plate tests.

indicates the test materials and conditions. JIS SUS 304 stainless steel was used for the test material instead of JIS SUS 420J2 stainless steel (the shaft material) due to its easy preparation. JIS SUS 304 stainless steel was verified in advance to have as large oil wettability as JIS SUS 420J2 stainless steel by measuring the contact angles of the oil. The smallest load (1.6 N) the tester used could make was chosen to prevent the solid-solid contact as much as possible.

Figure 12 shows the time evolution of the friction coefficient of the initial four reciprocations for the PTFE-coated and noncoated plates. A negative friction coefficient denotes the reverse sliding direction. Both shafts showed the friction coefficient of about 0.08 which were comparable to that of noncoated shaft shown in **Figure 5**. This means that the lubrication condition of the ball-on-plate tests was probably about the same as that of the bearing test of the noncoated shaft and the PTFE-coating showed no particular effect like oil-surface slippage on friction under such lubrication condition.

For testing the solid-lubricity of the PTFE-coated shaft under dry condition, “dried” bearing was made by ultrasonic cleaning of oil-impregnated sintered bearing in acetone for more than 10 minutes and tested by the test rig of **Figure 3**. Both noncoated and PTFE-coated shaft indicated the friction coefficient of 0.2–0.3 which means PTFE-coating had little effect on friction reduction under dry condition. From these results, the lubricity of the PTFE coating was presumed not to contribute to the friction reduction in the bearing test.

4.4 Mechanism to retain the oil droplets in the bearing clearance

In this section, the mechanism that caused the difference in oil amount in the bearing clearance will be discussed. Oil droplets in the bearing clearance will be modeled as micro-liquid bridges between slightly tilted plates. This modeling is appropriate because the angle between the shaft and bearing surfaces is usually very small.

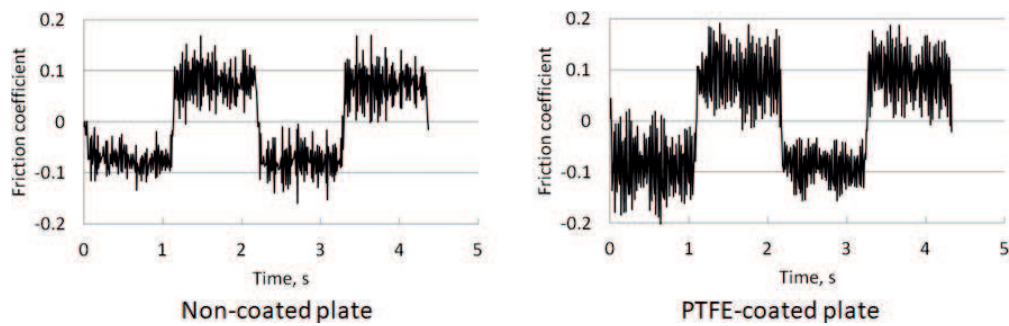


Figure 12.
Friction coefficient of ball-on-plate tests.

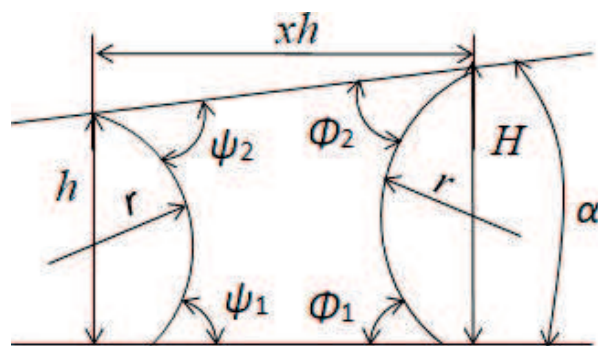


Figure 13.
 Liquid bridge between tilted plates.

Figure 13 illustrates the drum-formed liquid bridge between tilted plates. The meniscus radius r in **Figure 13** is expressed by Eq. (5) when the radius of the drum (liquid bridge thickness) is much larger than that of the meniscus and the effect of gravity is ignorable [18].

$$r \approx -\gamma/\Delta p = \text{const in the meniscus} \quad (5)$$

r is constant for a certain liquid bridge and the following relation holds geometrically:

$$H/h = \{ \cos \phi_1 + \cos(\phi_2 + \alpha) \} / \{ \cos \psi_1 + \cos(\psi_2 - \alpha) \} = 1 + x \tan \alpha \quad (6)$$

where x is the aspect ratio of the liquid bridge (thickness/height) assuming α is small. To satisfy this relation, contact angles have to vary according to the tilt angle and liquid bridge thickness.

The stability of liquid bridges between plates has been studied by several researchers [19–21]. According to these studies, the liquid bridge between parallel plates with a fixed contact angle between the liquid and the surface becomes unstable (which means a significant change of the liquid bridge in configuration and position) when one of the plates was tilted, even by a small amount [21]. This is because it is impossible to satisfy above relationship for the liquid-bridge with fixed contact angle.

Usually, contact angles could vary between receding and advancing contact angles, which is called contact angle hysteresis [22, 23], and the variable range depends on the liquid and surface material. According to the measuring method described in [22], the advancing angles were measured to be about 15 and 45°, and the receding angles were about 12 and 12.5° for noncoated and PTFE-coated plates, respectively. These results mean that contact angles could be in the following range: $12.5^\circ \leq \phi_1, \phi_2, \psi_1, \psi_2 \leq 45^\circ$ for the PTFE-coated plate.

Assume that these contact angles could be applied to the liquid bridges. $x = 3$, $\phi_1 = \phi_2 = 12^\circ$, and $\psi_1 = \psi_2 = 15^\circ$ for the noncoated plate combination according to the above measured values, then $\alpha \approx 0.22^\circ$ from Eq. (6). In the same way, for the PTFE-coated plate combination, $x = 3$, $\phi_1 = \phi_2 = 12.5^\circ$, and $\psi_1 = \psi_2 = 45^\circ$, then $\alpha \approx 5.7^\circ$. For larger α , liquid bridges become unstable. To verify this calculation, liquid bridge behavior was observed between plates with a 0.5-mm gap. A photo example of the test configuration and a schematic of the tester were shown in **Figure 14**. The bright line and blue two spots on the liquid bridge were the reflection of background and illumination lamp. The plates are initially set in parallel, and then rotated around the bottom center of the liquid bridge in steps of 0.5°. As shown in the figure, x could be read about 3.

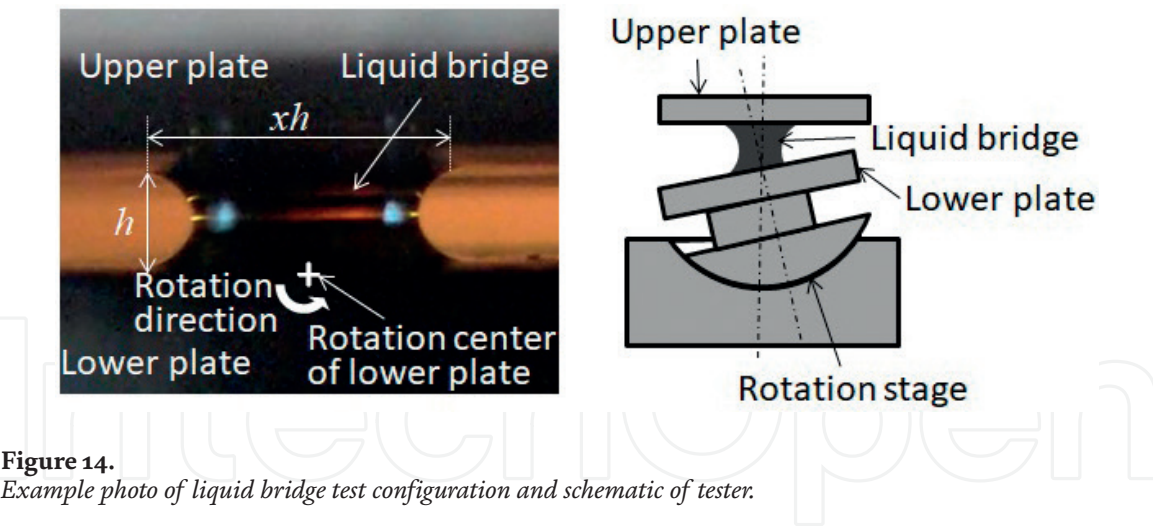


Figure 14.
Example photo of liquid bridge test configuration and schematic of tester.

For the noncoated upper and lower plate combination, the liquid bridge flowed in the narrower gap direction as soon as the tilt started. This means that the liquid bridge became unstable at a tilting angle less than 0.5° . For the PTFE-coated upper and lower plate combination, the liquid bridge flowed at tilting angles of $4\sim 6.5^\circ$ in several attempts. These results indicate that Eq. (6) is applicable for these conditions though Eq. (6) is not accurate, particularly when liquid bridge thickness is small, because the meniscus curve does not hold an arc shape but a more complex one (e.g., nodoid shape [20]).

We then applied Eq. (6) to the bearing clearance to estimate the possible maximum size of the oil droplet for the position in the clearance. The lower and upper plates can be considered to be the shaft and the bearing, respectively. The bearing surface has wettability similar to that of the noncoated shaft, which was roughly confirmed by oil droplet contact angle measurements. $\varphi_1 = \varphi_2 = 12^\circ$, $\psi_1 = \psi_2 = 15^\circ$ for noncoated shaft and $\varphi_1 = 12^\circ$, $\varphi_2 = 12.5^\circ$, $\psi_1 = 15^\circ$, and $\psi_2 = 45^\circ$ for PTFE-coated shaft, respectively, and $\tan\alpha = dh/d(R\theta)$ were used for the calculation. **Figure 15** shows the calculated critical oil bridge thickness (xh), that is, the largest possible size of oil droplets in the bearing clearance.

From **Figure 15**, the PTFE-coated shaft indicated larger critical oil bridge thicknesses and could retain much larger oil droplets in the bearing clearance than those

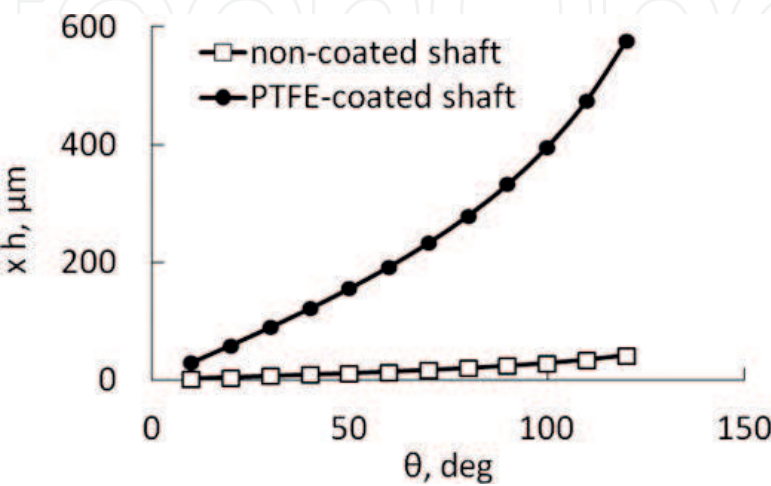


Figure 15.
Critical oil bridge thickness xh .

for the noncoated shaft. This effect may yield the results shown in **Figures 6** and **7** and lead to an oil-rich condition for the PTFE-coated shaft.

In addition to large oil droplets, clear movement of the oil droplets in the bearing clearance with shaft rotation was observed for the PTFE-coated shaft, as described in Section 4.2. This circulative movement in the clearance would induce the oil exudation from the bearing body probably contributing to large oil amount.

To investigate the movement of the oil droplets, the dragging effect of the oil droplets by the PTFE-coated shaft was examined by simple tests shown in **Figure 16**. An oil droplet was bridged between the parallel plates with 1-mm gap, and the upper plate was moved in parallel to the lower plate. The plates were SUS304 stainless steel and the upper plate of **Figure 16(a-1)** and **(a-2)** was PTFE-coated. The upper plates moved to the right by a distance of about 3 mm from the position of **Figure 16(a-1)** and **(b-1)** to the position of **Figure 16(a-2)** and **(b-2)**, respectively.

As can be seen from **Figure 16**, the PTFE-coated plate dragged the oil droplet firmly while the bare stainless plate did a little.

Figure 17 indicates the relationships between the upper plate travel distance and that of oil droplet. The oil droplet appears to stick to the PTFE-coated plate and to slip on the bare plate. This property may have caused the oil droplet circulation in the bearing clearance for the PTFE-coated shaft.

These phenomena would be a matter of energy but could also be explained by contact angle hysteresis. When the plate began to move, the oil droplet had to be deformed to retain the adhesion and the contact angle changed. As allowable contact angle range for the bare plate was much smaller than that of the PTFE-coated

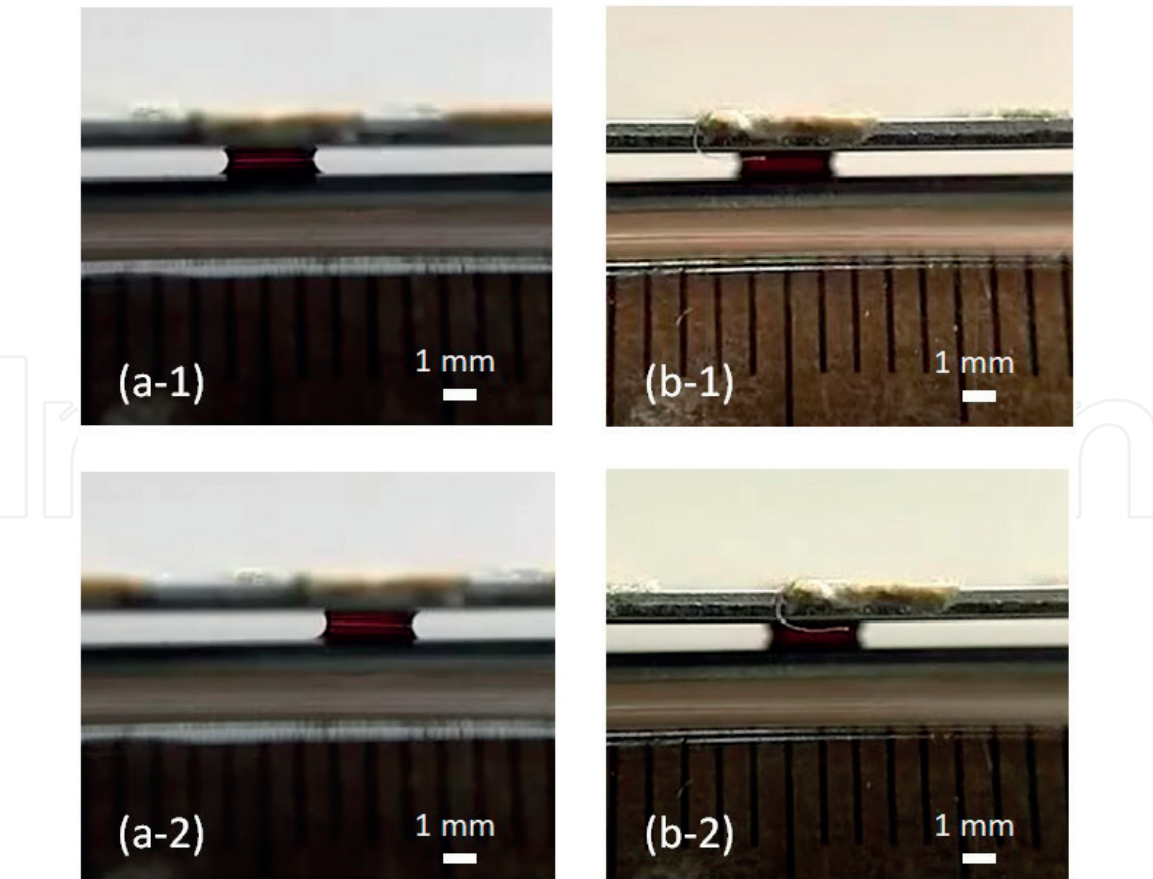


Figure 16.
Photos of oil droplet dragging test. (a-1) PTFE coated upper plate, original position. (a-2) 3 mm moved position. (b-1) Bare plate, original position. (b-2) 3 mm moved position.

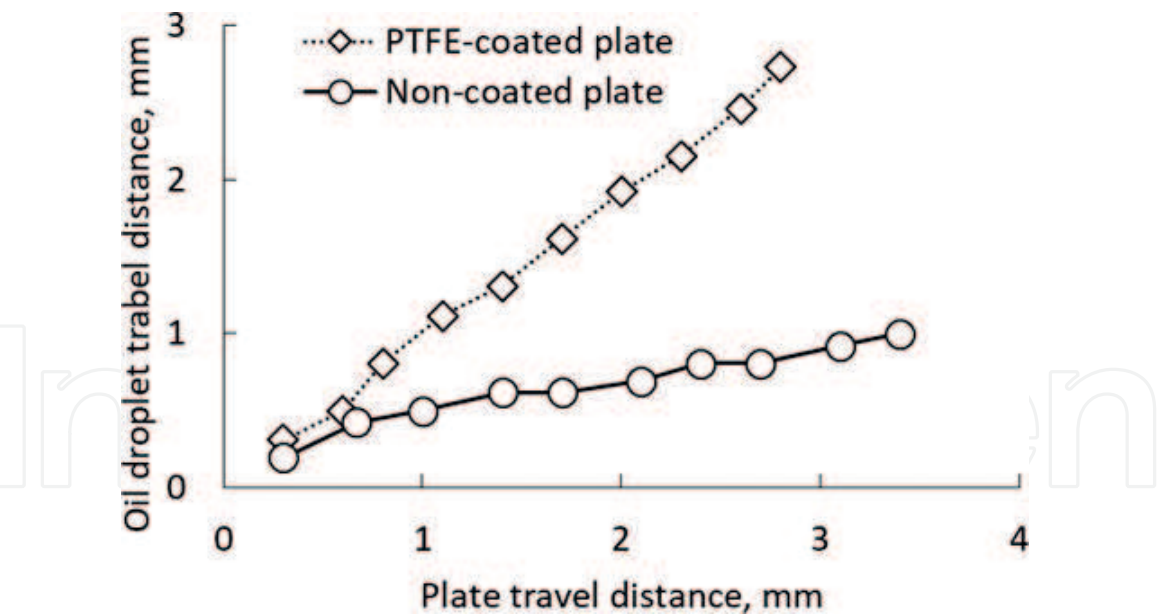


Figure 17.
Relationships between the upper plate travel distance and that of oil droplet.

plate, the interface between the oil droplet and the bare plate became unstable faster and caused to slip.

5. Conclusions

The oil-impregnated sintered bearing with PTFE-coated shaft showed lower friction than that with the noncoated (bare metal) shaft. The PTFE-coated shaft was found to retain a larger amount of oil droplets in the bearing clearance than the noncoated shaft and make secure oil circulation in the clearance. These effects would yield the oil-rich and better lubrication condition leading to lower friction of the PTFE-coated shaft.

The lower friction of the PTFE-coated shaft is attributed to the lower wettability to the impregnated oil than that of the noncoated shaft. Large contact angle hysteresis concomitantly with the low wettability makes it possible to retain larger oil droplets in the bearing clearance. The low wettable surface drags the oil droplets firmer than the high wettable surface, which generates the secure oil circulation in the bearing clearance for the PTFE-coated shaft.

Low wettability is often associated with a large contact angle hysteresis but probably it is not always the case. Therefore, note that probably the results of this study are not applicable to all kinds of low wettable shafts. The large contact angle hysteresis of the PTFE-coated shaft could also be caused by nonuniformity of the PTFE transfer film due to our rough production method [21].

However, generally speaking, using low wettable shafts must be one of the effective means to improve the lubrication condition and reduce the friction of oil-impregnated sintered bearings, though PTFE transfer film coating, which we used as low wettable coating in this study, is not wear-resistant and not a proper material for practical uses.

Acknowledgements

I would like to thank Fumiaki Katagiri and Yuta Kawabe, the former students of Institute of Technologists, for their devoted effort to the experiments.

Notes

Most of the content of this chapter is based on Ref. [5].

IntechOpen


IntechOpen

Author details

Naofumi Hiraoka
Institute of Technologists, Gyoda, Saitama, Japan

*Address all correspondence to: hiraoka@iot.ac.jp

IntechOpen

© 2018 The Author(s). Licensee IntechOpen. This chapter is distributed under the terms of the Creative Commons Attribution License (<http://creativecommons.org/licenses/by/3.0>), which permits unrestricted use, distribution, and reproduction in any medium, provided the original work is properly cited. 

References

- [1] Watanabe T. Present status of powder metallurgy in Japan. *The International Journal of Powder Metallurgy & Powder Technology*. 1980;**16**(3):249-253. (in Japanese)
- [2] Watanabe T. Porous sintered bearings. *Journal of the Japan Society of Powder and Powder Metallurgy*. 2001;**48**(9):769-776. (in Japanese). DOI: 10.2497/jjspm.48.769
- [3] Porite Corporation Product Information [Internet]. Available from: <http://www.porite.co.jp/product/example01.html> [Accessed: 30-07-2018]
- [4] Tanabe S. Energy saving tribology in impregnated sintered bearings. *Journal of Japanese Society of Tribologists*. 2006;**51**(5):353-358. (in Japanese)
- [5] Hiraoka N, Katagiri F, Kawabe Y. Effects of shaft surface wettability on the friction of oil-impregnated sintered bearings—Effect of contact angle hysteresis. *Tribology Online*. 2016;**11**(2):403-409. DOI: 10.2474/trol.11.403
- [6] Kaneko S. Porous oil bearings. *Journal of Japanese Society of Tribologists*. 1993;**38**(9):773-778. (in Japanese)
- [7] Quan Y-X, Ma J, Tian Y-G, Zhou G-R, Shi G-Y, Wang G-L. Investigation of sintered bronze bearings under high-speed conditions. *Tribology International*. 1985;**18**(2):75-80. DOI: 10.1016/0301-679X(85)90033-7
- [8] Sauer CH, Schatt W, Friedrich E. High performance Cu-basis PM bearings. In: *PM into the 1990s. International Conference on Powder Metallurgy*. 2. London. 1990. pp. 422-425
- [9] Choo JH, Glovnea RP, Forrest AK, Spikes HA. A low friction bearing based on liquid slip at the wall. *Journal of Tribology*. 2007;**129**(3):611-620. DOI: 10.1115/1.2736704
- [10] Ohmori H, Katahira K, Mizutani M. Functionalization of stainless steel surface through mirror-quality finish grinding. *CIRP Annals*. 2008;**57**(1):545-549. DOI: 10.1016/j.cirp.2008.03.131
- [11] Jap Soc Tribol. *Tribology Handbook*. Tokyo: Yokendo; 2001. pp. 744-747. (in Japanese)
- [12] Tanaka K, Miyata T. Studies on the friction and transfer of semicrystalline polymers. *Wear*. 1977;**41**(2):383-398
- [13] Wheeler DR. The transfer of polytetrafluoroethylene studied by X-ray photoelectron spectroscopy. *Wear*. 1981;**66**(3):355-365. DOI: 10.1016/0043-1648(81)90128-9
- [14] Lauer JL, Bunting G, Jones WRJR. Investigation of frictional transfer films of PTFE by infrared emission spectroscopy and phase-locked ellipsometry. *Tribology Transactions*. 1988;**31**(2):282-288. DOI: 10.1080/10402008808981824
- [15] Raman R, Babu LV. Tests on sintered bearings with reduced oil contents. *Wear*. 1984;**95**:263-269. DOI: 10.1016/0043-1648(84)90141-8
- [16] Leger L, Hervert H, Pit R. Friction and flow with slip at fluid-solid interfaces. *ACS Symposium Series*; **2001**:154-167
- [17] Voronov RS, Papavassiliou DV. Review of fluid slip over superhydrophobic surfaces and its dependence on the contact angle. *Industrial and Engineering Chemistry Research*. 2008;**47**:2455-2477. DOI: 10.1021/ie0712941
- [18] Taura H, Kaneko S. Meniscus forces of liquid bridge between two

parallel planes (comparison between exact solution and approximations). Transactions of the JSME. 2012;**78**(790):331-342. (in Japanese). DOI: 10.1299/kikaic.78.2266

[19] Chen T-Y, Tsamopoulos JA, Good RJ. Capillary bridges between parallel and non-parallel surfaces and their stability. Journal of Colloid and Interface Science. 1992;**151**(1):49-69. DOI: 10.1016/0021-9797(92)90237-G

[20] Langbein D. Stability of liquid bridges between parallel plates. Microgravity Science and Technology. 1992;**5**(1):2-11

[21] Concus P, Finn R. Discontinuous behavior of liquids between parallel and tilted plates. Physics of Fluids. 1998;**10**(1):39-43. DOI: 10.1063/1.869547

[22] Gennes P-G, Brochard-Wyart F, Quere D. Gouttes, Bulles, Perles et Ondes. Kyoto: Yoshioka Shoten; 2012. pp. 67-68. (Japanese Edition)

[23] Adamson AW, Gast AP. Physical Chemistry of Surfaces. New York: John Wiley & Sons; 1997. pp. 355-362